Aiglon, a magnetic spectrometer for low energy electrons

R. Battiston[a,b], W.J. Burger[*,a], A. Ostaptchouk[c], S. Schael[c]

[a] *INFN Sezione di Perugia, I-06100 Perugia, Italy*
[b] *Dipartimento di Fisica, Università di Perugia, I-06100 Perugia, Italy*
[c] *I. Physikalisches Institut B, D-52056 RWTH Aachen, Germany*

Abstract

The magnetic spectrometer is designed to detect low energy electrons (5-50 MeV) with good energy (10%) and angular ($< 5°$) resolutions, and sufficiently large acceptance ($10\,\mathrm{cm}^2\mathrm{sr}$), to monitor short term changes of the trapped particle population in the Earth's magnetic field. The influence of multiple Coulomb scattering is reduced by active collimation, filter planes composed of edgeless silicon microstrip detectors. The incident and exit particle trajectories are reconstructed in four planes of scintillating fibers. The spectrometer is a digital device in the sense that the notion of sampling is omnipresent: at the level of the filter plane design to suppress large angle multiply-scattered electrons, and at the level of the frontend electrons, where silicon photomultipliers (SiPM) are used.

Key words: charged particle spectrometers; tracking and position sensitive detectors; spaceborne and space research instruments

Introduction

The scientific goal is to measure low energy electrons and protons with good energy and angular resolutions in order to study the behavior of the trapped particle populations with respect to disturbances of solar, meteorological, seismic and anthropogenic origin. The behavior of the particles in the Earth's magnetic field are characterised by their rigidity and pitch angle. The latter requires a position measurement, whose resolution in the desired energy range is limited by multiple Coulomb scattering. For electrons, the presence of active collimator planes results in a good rigidity resolution with a magnetic spectrometer. The "open" design allows a measurement of non-relativistic protons (30-500 MeV) with good energy resolution (2-8%) *via* time of flight (50 ps resolution).

Principle of Operation

The rigidity is determined by a measurement of the incident and exit directions in six tracking planes. The planes closest to the magnet are segmented filters. The dimensional parameters relevant for the performance are presented in fig. 1.

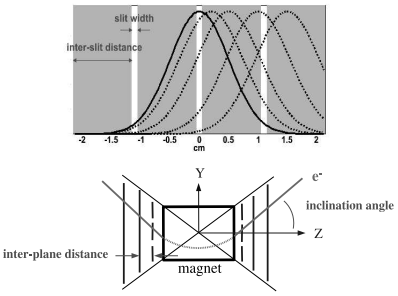

Figure 1: For a given inter-plane distance, the slit width of the filter planes should be smaller than the projected track error in the plane (gaussian), and the inter-strip distance sufficiently large to limit contamination from large scattering angles.

When the particle passes by a slit in the filter, its direction is reconstructed using the closest predicted slit position and the position recorded in the nearest tracking plane. For events with no recorded hits in the filter planes (2-slit), both the incident and exit directions are defined in this manner. In the case of 1-slit events, a three point reconstruction is made to determine the radius of curvature (fig. 2).

*corresponding author

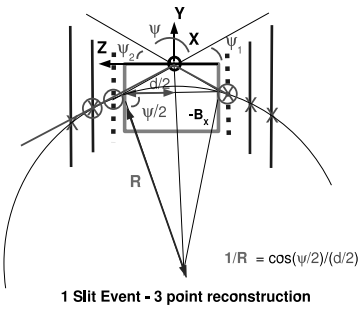

Figure 2: A 1-slit event, the deflection angle in the magnetic field is defined by three points: the closest predicted slit position in the upstream filter plane, the hit in the nearest upstream fiber plane and the hit in the downstream filter plane.

The track projection error at the filter planes as a function of the electron kinetic energy, and the electron 2-slit rigidity resolution, are shown in fig. 3 for two inter-plane distances. The results are obtained with a Geant3 [1] Monte Carlo simulation. The open circles in fig. 3 indicate the presence of multiple slit contributions; the corresponding reconstructed rigidity distributions between 8 and 50 MV are shown in fig. 4.

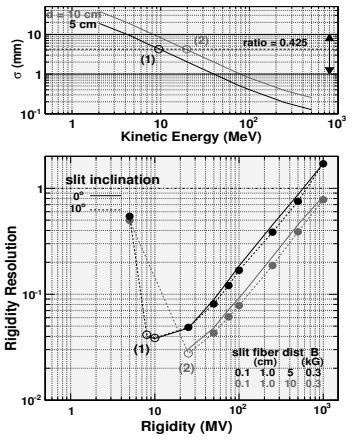

Figure 3: Track projection error at the filter planes (top); 2-slit rigidity resolution with a 0.3 kG field, a slit width of 1 mm, an inter-slit distance of 1 cm and inter-plane distances of 5 and 10 cm (bottom). The optimal resolutions, (1) and (2), correspond to a slit-width-separation ratio of 0.425; the optimal performance shifts toward higher rigidity with increasing inter-plane distance.

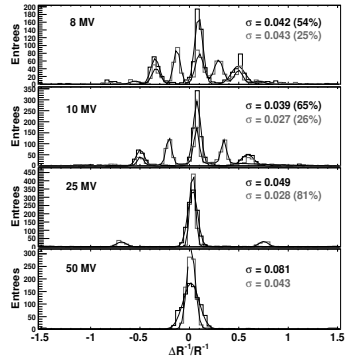

Figure 4: The reconstructed rigidity distributions with inter-plane distances of 5 (black) and 10 (gray) cm. The widths of the central gaussian, and in the presence of multiple gaussian (slit) contributions, the area of the central gaussian with respect to the total area of the combined fit are quoted for electron rigidities of 8, 10, 25 and 50 MV. The central gaussian widths are reported in fig. 3; at the lowest rigidity (5 MV), a single gaussian was used to quantify the width of the multiple peak distribution.

Technologies Employed

The scintillating fiber tracker planes are composed of 250 μm fibers which are glued together to form a four-fiber thick half-plane. The SiPM arrays are attached to the fibers so that each readout channel receives the signals of the pixels covering a four-layer thick, 250 μm wide column. The fibers centers of alternating layers are displaced by 125 μm. The expected resolution is 40 μm [2]; the simulation results were obtained with a resolution of 80 μm for the fiber/filter planes.

The fibers of two half-planes are oriented orthogonally. With a density of four channels per mm per coordinate, the total number of readout channels of the fiber tracker is 7884. The non-bending coordinate half-plane of the outermost planes consists of finely segmented scintillator bars read out with SiPM's, which provide the trigger and proton time of flight.

In the simulation, the filter planes are composed of $229 \times 10 \times 1.0\,\mathrm{mm}^3$ fiber panels separated by 1 mm. In practice, edgeless silicon microstrip detectors represent an nearly ideal choice: a negligible dead region at the sensor edge ($< 5\,\mu$m), high efficiency ($\sim 99\,\%$) and a thickness ($\leq 300\,\mu$m) [3], which offers a superior aspect ratio, slit width-to-depth, for the acceptance at lowest rigidities (*cf.* fig. 3). The avantages largely compensate the $\sim 15\%$ increase in radiation length.

Two NdFeB cylindrical magnets, with an inner diameter of 20 cm, a length of 24 cm and a mass of 6.49 kg,

have been constructed. [1] A 0.64 kG field is orientated perpendicular to the axis of the cylinders, while the net dipole moment of the magnets is zero [4].

The satellite payload will include two spectrometers to view in orthogonal directions. With a near polar orbit, the 0° detector samples 0° (90°) pitch angle at the pole (equator), while the 90° detector views in permanence in the direction perpendicular to the local field line.

Expected Performance

The 0, 1 and 2 slit electron rigidity resolutions are presented in fig. 5 for a 0.60 kG field. The corresponding acceptances between 10-50 MeV are 130, 10 and 0.35 cm^2sr respectively, for the 20 cm inner diameter magnet.

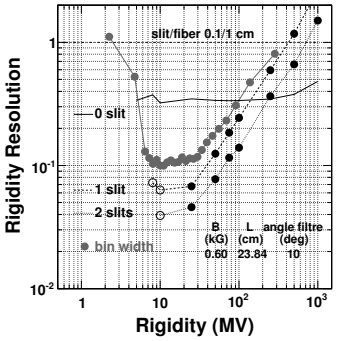

Figure 5: The 0, 1 and 2 electron rigidity resolutions. The bin widths, normalised with the rigidity value of the bin center, represent a more realistic estimation of the 1-slit resolution taking into account the electron energy spectra (E^{-3}), i.e. the migration between bins due to the difference between generated and reconstructed rigidities.

The 1-slit performance is also quoted in terms of bin width of the reconstructed rigidity (energy) spectra, divided by the rigidity of the center of the bin. In this case, electrons were generated over the full geometric acceptance using a power law in energy E^{-3} between 2-200 MeV [5]. The bin widths were chosen to limit the migration to adjacent bins due to the difference between the generated and reconstructed rigidities to less than 50%. In principle, the reconstructed rigidity distribution may be unfolded to correct for the effect of the experimental resolution on the reconstructed rigidities [6].

[1] the Institute of Electrical Engineering, Chinese Academy of Sciences, Beijing, China

Aiglon is compared with existing satellite payload, solid-state particle detectors in table. 1. The solid-state devices use the relation energy-range to obtain the low energy particle spectra from measurements of specific and total energy loss. The pitch angle is defined by the axis of the field-of-view. With Aiglon, the pitch angles in the field-of-view are measured with resolutions of 4° and 0.8° at the lowest electron and proton energies respectively.

Table 1: Comparison with existing satellite payload, solid-state particle detectors. The quoted "geometric factor" of the magnetic spectrometer includes the effect of the field. The Aiglon geometric factors and angular resolutions for electrons and **protons** are indicated separately.

detector	geometric factor cm^2sr	aperture	pitch angle	range	
				electron *MeV*	proton *MeV*
SAMPEX	1.7	58°	0-90°	1-4	19-28
PET [7]				4-20	28-64
DEMETER	1.2	32°	90°	0.07-2.4	
IDP [8]					
NOAA	0.1	30°	0-90°	0.03- 2.5	0.03-6.9
MEPED [9]			90°		
AIGLON	10	40°	0-90°	5-50	30-500
	75-130	$\Delta 4°$,$\mathbf{\Delta 0.8°}$	90°		

Conclusion

The proposed magnetic spectrometer represents an interesting alternative to the solid-state devices currently used for low energy particle detection in space. With an approach incorporating state-of-the-art detection techniques, the device provides good energy and angular resolutions, and comparatively larger acceptances, for electrons and protons.

References

[1] R. Brun et al.,CERN Report DD/EE/84-1, revised 1987.
[2] H. Glast et al., Nucl. Instr. and Meth. A 581 (2007) 423-426.
[3] V. Avati et al., Nucl. Instr. and Meth. A 518 (2004) 264-267.
[4] M. Aguilar et al., Phys. Reports 366 (2002) 331-405.
[5] X. Li et al., Geophys. Res. Lett., Vol. 24, No. 8 (1997) 923-926.
[6] G. D'Agostini, Nucl. Instr. and Meth. A 362 (1995) 487-498.
[7] W.R. Cook et al., IEEE-Trans. on GeoScience and Remote Sensing, Vol. 31, No. 1 (1993) 565-571.
[8] J.A. Sauvaud et al., Planetary and Space Science 54 (2006) 502-511.
[9] National Oceanic and Atmospheric Administration Technical Memorandum, version 1.4, January (2004).